Available online at www.sciencedirect.com
ScienceDirect
Carbohydrate Research 342 (2007) 1350–1356
Carbohydrate RESEARCH

B3LYP/6-311++G** study of structure and spin–spin coupling constant in heparin disaccharide

M. Hricovíni,[a,*] E. Scholtzová[b] and F. Bízik[c]

[a]Institute of Chemistry, Slovak Academy of Sciences, 845 38 Bratislava, Slovakia
[b]Institute of Inorganic Chemistry, Slovak Academy of Sciences, 845 36 Bratislava, Slovakia
[c]Institute of Virology, Slovak Academy of Sciences, 842 45 Bratislava, Slovakia

Received 21 December 2006; received in revised form 16 March 2007; accepted 19 March 2007
Available online 24 March 2007

Abstract—Structures of heparin disaccharide have been analyzed by DFT using the B3LYP/6-311++G** method. The optimized geometries of two forms of this disaccharide, differing in the conformation ($^1C_4$ and $^2S_0$) of the IdoA2S residue, confirmed considerable influences of the sulfate and the carboxylate groups upon the pyranose ring geometries. The computed energies showed that disaccharide having the $^1C_4$ form of the IdoA2S residue is more stable than that with the $^2S_0$ form. Interatomic distances, bond and torsion angles showed that interconversion of the IdoA2S residue results in geometry changes in the GlcN,6S residue as well. Three-bond proton–proton and proton–carbon spin–spin coupling constants computed for both forms agree with the experimental data and indicate that only two chair forms contribute to the conformational equilibrium in disaccharide. Influences of the charged groups upon the magnitudes of spin–spin coupling constants are also discussed.

Keywords: Heparin; Disaccharide; Conformation; DFT calculations; NMR coupling constants

1. Introduction

Glycosaminoglycans (GAGs) are complex linear polysaccharides, which are constituted by disaccharide units of an uronic acid and hexosamine. GAGs, such as heparin, are involved in various important biological functions and have been widely studied.[1–5] Heparin is made up by uronic acid (glucuronic acid or iduronic acid) and hexosamine, predominantly 2-amino-2-deoxy-D-glucose. These residues are substituted to various degree by O- or N-sulfated (O-SO_3^- or N-SO_3^-) groups. Pyranose ring conformations, as well as pendant groups, have been the subject of particular interest as they play key roles in intermolecular interactions with proteins.[1,4–7] NMR,[6–8] and theoretical analyses[9–12] showed that iduronic acid, and especially 2-O-sulfated derivative (IdoA2S), is a flexible residue in heparin and heparin-derived oligosaccharides. Three forms, $^1C_4$, $^4C_1$, and $^2S_0$, are largely present in conformational equilibrium of this residue. The populations of these conformers depend upon the structure of neighboring units, type of counterions and concentration. Theoretical analysis, together with experimental NMR spin–spin coupling constants and NOEs, enabled estimation of conformer populations in different oligo- and polysaccharides.[2,3,7,8,13–18]

As mentioned, heparin is heterogeneous polysaccharide, however, it is prevalently constituted from repeating disaccharide units GlcN,6S-IdoA2S linked with α-(1→4) linkage. This paper reports results from DFT calculations of the methyl glycoside of heparin disaccharide (GlcN,6S-IdoA2S-OMe) using the B3LYP/6-311++G** method. The optimized geometries were carried out for two forms of this disaccharide, differing in the conformations ($^1C_4$ and $^2S_0$) of the IdoA2S residue. Previous analyses showed that high level basis sets, including diffuse functions, are important when dealing with saccharides bearing sulfate and carboxylate groups.

* Corresponding author. Tel.: +421 2 59410323; fax: +421 2 59410222; e-mail: hricovini@savba.sk

0008-6215/$ - see front matter © 2007 Elsevier Ltd. All rights reserved.
doi:10.1016/j.carres.2007.03.020

Recent DFT calculations at the B3LYP/6-311++G** level of theory gave reliable energies and geometries for several carbohydrates.[19–22] Well-refined structures are essential for calculations of other theoretical data, such as NMR parameters. Calculations on structurally similar compounds,[23–25] obtained using the B3LYP/6-311++G** and B3LYP/6-31+G* basis sets, enabled calculations of geometries, energies and NMR parameters. Computed geometries were not comparable in several parameters with those previously derived by molecular mechanics or dynamics and prompted us to extent these calculations on heparin disaccharide. In addition, DFT-based NMR spin–spin coupling constants were compared with experimental values measured in the same compound.

2. Computational methodology

The geometry of heparin disaccharide [methyl *O*-(2-deoxy-2-sulfamino-6-*O*-sulfo-α-D-glucopyranosyl)-(1→4)-2-*O*-sulfo-α-L-idopyranosideuronate tetrasodium salt; GlcN,6S-IdoA2S-OMe] molecule has been completely optimized with the JAGUAR program[26] using density functional theory (DFT)[27] with Lee–Young–Parr (B3LYP)[28] correlation functional and the 6-311++G** basis set. The IdoA2S residue was considered in two conformers ($^1C_4$ and $^2S_0$, Scheme 1) whereas the GlcN,6S residue was in the $^4C_1$ conformation regardless of the IdoA2S form. Starting geometries for optimization were obtained by B3LYP/6-31+G* method.[29] Hybrid functionals with the Slater local functional/Becke88 nonlocal gradient correlation[30] and Vosko–Wilk–Nusair local functionals[31] were used. Geometry optimizations were obtained with the gradient optimization routine, the convergence criteria were set to 1×10^{-6}. Geometry was optimized without treatment of solvent effects as previous data showed that continuous solvent models do not reliably account for the reorganization energy term in this type of compounds.[24] NMR proton–proton and proton–carbon spin–spin coupling constants were computed with the GAUSSIAN 03 program[32] at the B3LYP/DGDZVP level of theory.[33]

3. Results and discussion

3.1. Geometry

As mentioned, the iduronate unit adopts various conformations in heparin-like oligosaccharides. Computed geometry of two forms of heparin disaccharide, differing each other in the IdoA2S residue conformations, are listed in Tables 1–3. Computed data indicate that the bond lengths (Table 1) vary with the form of the IdoA2S ring not only in the IdoA2S residue but in the GlcN,6S residue as well. Interatomic separations in the IdoA2S ring are comparable with the previously determined theoretical[24] and experimental[34] data of the structurally related compounds. The largest differences within the IdoA2S residue are, as expected, in the C1–O1 (0.036 Å), the S(2)–O and C6–O distances. Variations in both S(2)–O and C6–O separations are due to the presence of sodium ions in different positions with respect to oxygen atoms. The interatomic distances in the 2-*O*-sulfate group reveal that both S2–O22 and S2–O23 are longer (1.493 and 1.497 Å) than the S2–O21 distance (1.443 Å) in the $^2S_0$ conformer. The bond lengths and atomic charges (−0.594 and −0.622) on both O22 and O23 suggest the resonance bond character of the S2–O22 and S2–O23 linkages whereas the S2–O21 bond is double bond. In the $^1C_4$ conformer, however, O21 and O22 oxygens are more negatively charged (−0.550 and −0.656) than O23 and the S2–O23 distance

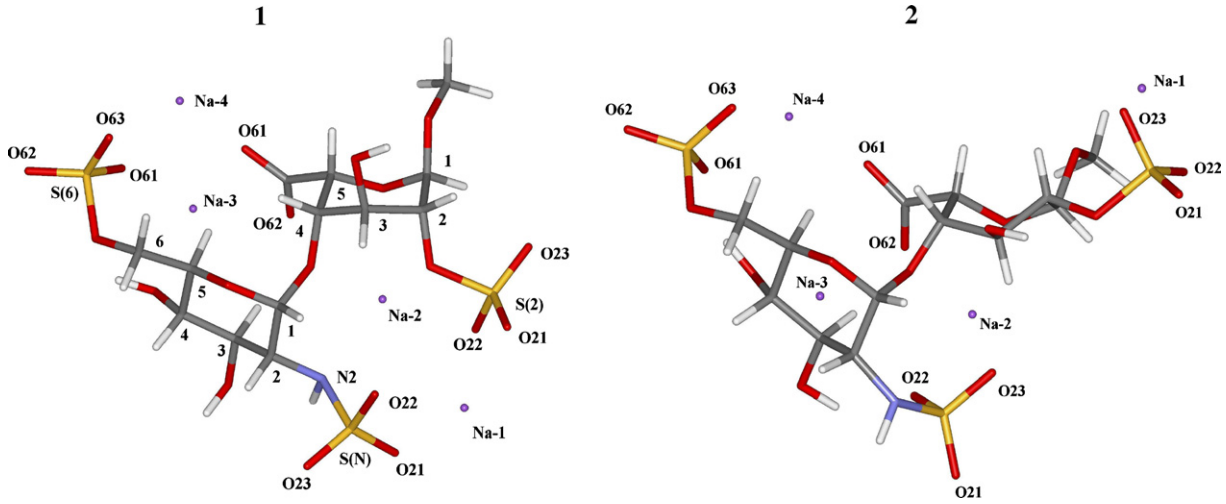

Scheme 1. Schematic representations of heparin disaccharide. Two forms (**1** and **2**) correspond to different conformations ($^1C_4$ and $^2S_0$) of the IdoA2S residue. The GlcN,6S residue is in the $^4C_1$ form.

Table 1. Selected optimized (B3LYP/6-311++G**) interatomic distances (in Å) in heparin disaccharide

Residue	Bond	$^1C_4$	$^2S_0$
IdoA2S	C1–C2	1.536	1.540
	C2–C3	1.545	1.537
	C3–C4	1.546	1.538
	C4–C5	1.538	1.546
	C5–O5	1.432	1.447
	C1–O5	1.433	1.420
	C1–O1	1.392	1.428
	C5–C6	1.531	1.548
	C2–O2	1.431	1.424
	S2–O2	1.704	1.692
	S2–O21	1.474	1.443
	S2–O22	1.494	1.493
	S2–O23	1.456	1.497
	O22–Na1	—	2.277
	O23–Na1	—	2.254
	O1–Na1	—	2.374
	O21–Na1	2.339	—
	O22–Na1	2.476	—
	O5–Na2	2.689	2.346
	O2–Na2	2.380	—
	O62–Na2	—	2.300
	O62–Na3	—	2.331
	O61–Na4	2.143	2.165
	O61–Na3	2.409	—
	O62–Na3	2.415	—
	C6–O61	1.276	1.248
	C6–O62	1.243	1.262
	H1–H2	2.573	3.023
	H1–H3	4.238	2.859
	H2–H4	4.258	2.958
	H2–H5	3.894	2.509
GlcN,6S	C1–C2	1.540	1.541
	C2–C3	1.537	1.542
	C3–C4	1.523	1.527
	C4–C5	1.542	1.553
	C5–O5	1.430	1.437
	C1–O5	1.412	1.408
	C1–O1	1.423	1.423
	C5–C6	1.531	1.534
	C2–N2	1.473	1.461
	S(N)–N2	1.758	1.705
	S(N)–O21	1.488	1.455
	S(N)–O22	1.489	1.522
	S(N)–O23	1.463	1.487
	O21–Na1	2.356	—
	O22–Na1	2.328	—
	O1–Na2	2.358	2.941
	O22–Na2	—	2.333
	O23–Na2	—	2.268
	N2–Na2	2.506	—
	C6–O6	1.443	1.434
	O6–S6	1.678	1.664
	S6–O61	1.506	1.511
	S6–O62	1.444	1.444
	S6–O63	1.488	1.491
	O61–Na4	2.427	2.316
	O63–Na4	2.272	2.310
	O61–Na3	2.305	—
	O4–Na3	2.375	2.240
	O3–Na3	—	2.768
	H1–H2	2.442	2.534
	H2–H4	2.617	2.642
	H3–H5	2.716	2.780

Two conformers ($^1C_4$ and $^2S_0$) of the IdoA2S residue are considered. The GlcN,6S residue is in the $^4C_1$ form.

Table 2. Selected optimized and experimental bond angles (in degrees) in heparin disaccharide

Residue	Bond angle	$^1C_4$	$^2S_0$
IdoA2S	O5–C1–C2	109.1	111.8
	O5–C1–O1	113.3	109.6
	O1–C1–C2	109.1	109.8
	C5–O5–C1	112.1	112.8
	C1–C2–C3	113.7	110.0
	C1–O1–C_{Me}	114.2	112.6
	C2–O2–S2	122.7	119.6
GlcN,6S	O5–C1–C2	109.7	108.8
	O5–C1–O1	112.9	111.8
	O1–C1–C2	106.8	106.5
	C5–O5–C1	116.6	116.9
	C1–C2–C3	110.5	105.0
	C1–O1–$C4_{IdoA}$	120.1	120.0
	C2–N2–S(N)	113.3	127.3
	C5–C6–S(6)	111.8	114.0

Two conformers ($^1C_4$ and $^2S_0$) of the IdoA2S residue are considered. The GlcN,6S residue is in the $^4C_1$ form.

is shorter (1.456 Å). It also should be noted that the S2–O23 distance in the $^2S_0$ form is shorter than the S2–O21 bond in the chair form. This is due to the different coordination of Na-1 ion ($-SO_3^- \cdots Na^+ \cdots O1$) in the $^2S_0$ conformer with respect to the chair form (Scheme 1). Similarly, S(N)–O21 and S(N)–O22 separations are longer (1.488 and 1.489 Å) than the S(N)–O23 distance (1.463 Å) in the GlcN,6S residue ($^1C_4$ chair form of the IdoA2S). Even larger differences in bond lengths between the S=O double bond ($d_{S(N)-O21} = 1.455$ Å) and the other two bonds ($d_{S(N)-O22} = 1.522$ Å and $d_{S(N)-O23} = 1.487$ Å) in the NSO_3^- group were obtained for the $^2S_0$ form of the IdoA2S residue. The bond distance variations were analogous also in the 6-*O*-sulfate group. The above evidence of the two longer S–O bonds and one double bond in both NSO_3^- and OSO_3^- groups is in agreement with the published crystallographic data of N-sulfated glucosamine[34] where the measured S–O distance of the double bond was 1.446 Å.

Variations in bond angles (Table 2) were most significant in the pendant groups, for example, the bond angles C2–O2–S2 (IdoA2S) and C2–N2–S(N) (GlcN,6S) varied up to 14°. Within the pyranose rings, the largest changes were obtained in the anomeric part (e.g., O5–C1–O1, O5–C1–C2) in both residues. Interestingly, the glycosidic linkage bond angle ($C1_{GlcN,6S}$–O1–$C4_{IdoA2S}$) remained the same regardless of the IdoA2S form. The

Table 3. Selected optimized and experimental torsion angles (in degrees) in heparin disaccharide

Residue	Torsion angle	$^1C_4$	$^2S_0$
IdoA2S	O5–C1–C2–C3	−50	26
	C6–C5–O5–C1	170	164
	O5–C1–C2–C_{Me}	−75	−65
	C1–C2–C3–C4	42	−59
	C2–C3–C4–C5	−43	27
	C1–C2–O2–S1	77	84
	H1–C1–O5–C5	−179	159
	H1–C1–C2–C3	−164	−92
	H2–C2–C3–C4	166	63
	H3–C3–C4–C5	−162	−92
	H1–C1–C2–H2	72	147
	H2–C2–C3–H3	−74	−179
	H3–C3–C4–H4	79	148
	H4–C4–C5–H5	53	36
	H4–C4–O1–$C1_{Glc}$	−39	−44
GlcN,6S	O5–C1–C2–C3	57	67
	C6–C5–O5–C1	176	168
	O5–C1–O1–$C4_{IdoA}$	51	68
	C1–C2–C3–C4	−55	−62
	C2–C3–C4–C5	50	48
	C1–C2–O2–S1	87	−82
	H1–C1–O5–C5	−177	179
	H1–C1–C2–C3	173	−176
	H1–C1–O1–$C4_{IdoA}$	−67	−50
	H2–C2–C3–C4	61	51
	H3–C3–C4–C5	−69	−65
	H1–C1–C2–H2	55	68
	H2–C2–C3–H3	180	166
	H3–C3–C4–H4	170	172
	H4–C4–C5–H5	−167	−154

Two conformers ($^1C_4$ and $^2S_0$) of the IdoA2S residue are considered. The GlcN,6S residue is in the $^4C_1$ form.

values of torsion angles (Table 3) indicated that sulfate and carboxylate groups influenced the ring geometries of both pyranose rings and pendant groups in heparin disaccharide. Except of obvious differences in the IdoA2S residue 3D structure, there are also variations in the GlcN,6S residue. This comprises not only heavy atoms (e.g., variations in the torsion angle in the array O5–C1–C2–C3) but hydrogens as well. The differences up to 14° (H2–C2–C3–H3) are relatively large and result in different magnitudes of three-bond proton–proton coupling constants in the two disaccharide forms. Such an influence of the IdoA residue ring form upon the 3D structure of the GlcN,6S unit is remarkable. The effects of sulfate and carboxylate groups, counterions, and hydrogen bonds (see later discussion) thus results not only in conformational change of the IdoA residue but influence the structure of the GlcN,6S residue as well. Such effects are not that profound as in the iduronate unit but cannot be neglected and require further analysis in other heparin-like saccharides. As expected, ϕ, ψ torsion angles (H1–C1–O1–$C4_{IdoA2S}$, H4–C4–O1–$C1_{GlcN,6S}$) at the glycosidic linkage also varied with the IdoA2S ring form.

The coordination of sodium ions varied upon the IdoA2S ring forms. In the $^1C_4$ chair form, $Na1^+$ and $Na2^+$ were located between the *N*-sulfate and the 2-*O*-sulfate groups (Scheme 1). In the $^2S_0$ form, $Na1^+$ adopted quite different position among anomeric O1 oxygen and two oxygens from the 2-*O*-sulfate group. The distances between $Na1^+$ cations and adjacent oxygens are comparable to each other in both forms and are similar to experimentally observed sodium-to-oxygen distances.[34] It should be noted, that the starting positions (before geometry optimization) of $Na1^+$ cations were the same in both conformations. Sodium cation changed considerably its position during optimization in the $^1C_4$ chair form whereas $Na1^+$ remained close to the anomeric O1 in the $^2S_0$ form. Inspection of interatomic distances (Table 1) indicates that there are differences also in $Na2^+$ cations coordination. In the $^2S_0$ form, $Na2^+$ adopted position among O22 and O23 of the *N*-sulfate group, O62 (the carboxylate oxygen) and the O5 ring oxygen in the IdoA2S unit (Scheme 1). This differs from the chair conformation where $Na2^+$ cation was coordinated with O2 (IdoA2S) and N2 of the *N*-sulfate group. Differences were obtained also for intramolecular hydrogen bonds in the GlcN,6S residue. In the skewed conformation, both OH3 and OH4 had hydrogen bonds with the *N*-sulfate group (O22) and the 6-*O*-sulfate group (O61), respectively. Unlike this, OH4 had hydrogen bond with O6 in the GlcN,6S residue in the chair conformation. The above data show that the IdoA2S residue conformation considerably influences also the hydrogen bonds in the adjacent GlcN,6S unit.

Computed relative, zero-point vibrational (ZPVE), and corrected relative energies based on the B3LYP/6311++G** geometry optimization of heparin disaccharide conformers are in Table 4. The energy values indicate that the $^1C_4$ conformer is more stable than the skewed form. Significant populations of the $^1C_4$ form in conformational equilibrium have been obtained in previous DFT[24] and molecular mechanics study[9] in structurally related compounds. On the other hand, results of MD simulations[10] agreed with considerable interconversion among three forms ($^1C_4$, $^4C_1$, and $^2S_0$) of the iduronate ring. Computed energy values (Table 4) suggest that the $^1C_4$ form is nearly exclusively present

Table 4. Calculated relative (ΔE), zero-point vibrational (ZPVE), and corrected relative (ΔE_{corr}) energies (values in kcal/mol) based on the B3LYP/6311++G** geometry optimization of the heparin disaccharide

	$^1C_4$	$^2S_0$
ΔE	0[a]	24.346
ZPVE	249.536	249.925
ΔE_{corr}	0	24.735

Two conformers ($^1C_4$ and $^2S_0$) of the IdoA2S residue are considered.
[a] Energy: −3910.70734455.

in equilibrium. High population of the $^1C_4$ conformer agrees with experimental spin–spin coupling constants, however, the presence of the skewed form is also required to interpret the experimental data.

3.2. NMR spin–spin coupling constants

Computed three-bond proton–proton coupling constants in the H–C–C–H atom array ($^3J_{H–C–C–H}$) in heparin disaccharide are given in Table 5. In general, coupling constants depended upon torsion angles and vary within the interval between 1.61 and 11.34 Hz. In addition to obvious $^3J_{H–C–C–H}$ variations in the $^1C_4$ and $^2S_0$ conformations (IdoA2S residues), $^3J_{H–C–C–H}$ magnitudes also differed in the GlcN,6S residue. This finding was rather surprising as this residue was in the $^4C_1$ conformation regardless of the IdoA2S conformation. In fact, published experimental data indicated differences (in same cases quite considerable) in coupling constants magnitudes in various GAGs.[8] However, detailed analysis has not been performed. The present data clearly showed that the pyranose ring geometry of the glucosamine residue differed depending on the IdoA residue conformation. As already mentioned, the variation of the torsion angles were up to 14° (H2–C2–C3–H3) and consequently, the $^3J_{H–C–C–H}$ magnitudes varied considerably in some cases. For example, $^3J_{H-1,H-2}$ were 3.70 Hz ($^1C_4$) and 2.17 Hz ($^2S_0$), respectively. Similar large differences (9.20 and 7.66 Hz) were obtained for $^3J_{H-4,H-5}$. It should be also noted that the computed coupling constants were found comparable with those previously obtained in monosaccharide IdoA2SOMe[24] and the $^3J_{H–C–C–H}$ magnitudes varied within 1 Hz.

$^3J_{H–C–C–H}$ magnitudes indicate that atom electronegativities and the presence of charged groups considerably affect the values of coupling constants as well. $^3J_{H-4,H-5}$ coupling constant in the IdoA2S ($^1C_4$) is a good example of such influence. Its value (2.72 Hz) is comparable with the $^3J_{H-3,H-4}$ (2.54 Hz) but there is difference of about 25° in the torsion angles (Table 5). Such difference in geometry would suggest much bigger variations in the coupling constants magnitudes. Comparison of this coupling constant ($^3J_{H-4,H-5} = 2.72$ Hz) with $^3J_{H-1,H-2}$ in the GlcN,6S residue in the same compound **1** ($^3J_{H-1,H-2} = 3.70$ Hz) shows that nearly 1 Hz difference was obtained for coupling constants with comparable torsion angles (53° and 55°, respectively). Similar trends were also observed in monosaccharide IdoA2SOMe.[24]

Comparison of theoretical and experimental $^3J_{H–C–C–H}$ values[35] is shown in Table 6. Presented theoretical values were obtained as the best fit of varying conformer populations to experimental data. The ratio $^1C_4$:$^2S_0 = 79:21$ led to a very good agreement between theory and experiment and most of the computed coupling constants were within the experimental error. The largest differences were obtained for $^3J_{H-4,H-5}$ in both residues, however, the difference was larger (1.5 Hz) in the GlcN,6S residue. In fact, $^3J_{H-4,H-5}$ magnitudes in the GlcN,6S residues (corresponding to two forms of the IdoA2S) were relatively small (9.20 and 7.66 Hz, respectively) thought the torsion angles would suggest more than 1 Hz larger values.[25] The computed magnitudes seemed to be affected by other factors (C4–C5 bond lengths, charges, O5 lone pairs) than torsion angles exclusively, as already discussed in this and previous papers.[24,25]

Selected computed three-bond proton–carbon coupling constants ($^3J_{H–C–C–C}$ and $^3J_{H–C–O–C}$) are listed in Table 7. Both types of coupling constants follow the Karplus-type relationship, however, the influences of stereoelectronic effects are considerable in this type of coupling constants as well. For example, magnitudes of $^3J_{H-1,C-1,O-5,C-5}$ in compound **1** are 4.40 Hz (IdoA2S in the $^1C_4$ form) and 6.41 Hz in the GlcN,6S although the torsion angles are comparable (181° vs 183°). Differ-

Table 5. Computed three-bond proton–proton coupling constants (values in Hz) in heparin disaccharide

	Conformation	Residue	Array of atoms	Torsion angle	$^3J_{H–C–C–H}$
1	$^1C_4$	IdoA2S	H1–H2	72	1.61
			H2–H3	−74	2.60
			H3–H4	79	2.54
			H4–H5	53	2.72
	$^4C_1$	GlcN,6S	H1–H2	55	3.70
			H2–H3	180	11.34
			H3–H4	170	9.40
			H4–H5	−167	9.20
2	$^2S_0$	IdoA2S	H1–H2	147	5.41
			H2–H3	−179	11.15
			H3–H4	148	4.87
			H4–H5	36	5.09
	$^4C_1$	GlcN,6S	H1–H2	68	2.17
			H2–H3	166	11.03
			H3–H4	172	9.92
			H4–H5	−154	7.66

Two forms (**1** and **2**) correspond to different conformations ($^1C_4$ and $^2S_0$) of the IdoA2S residue. The GlcN,6S residue is in the $^4C_1$ form.

Table 6. Experimental (3rd column) and computed averaged ($^1C_4$:$^2S_0 = 79:21$) best-fit (4th column) three-bond proton–proton coupling constants (values in Hz) in heparin disaccharide

Residue	Array of atoms	$^3J_{H–C–C–H}$	
		Exp.[a]	Comp.
IdoA2S	H1–H2	2.3	2.4
	H2–H3	4.6	4.4
	H3–H4	3.4	3.1
	H4–H5	2.6	3.2
GlcN,6S	H1–H2	3.6	3.4
	H2–H3	11.4	11.3
	H3–H4	9.5	9.5
	H4–H5	10.4	8.9

[a] Taken from Ref. 35.

Table 7. Computed three-bond proton–carbon coupling constants (values in Hz) in heparin disaccharide

	Conformation	Residue	Array of atoms	$^3J_{H–C–X–C}$ Comp.
1	$^1C_4$	IdoA2S	H1–C1–O5–C5	4.40
			H5–C1–O5–C1	2.27
			H1–C1–C2–C3	2.35
			H3–C3–C2–C1	3.07
			H4–C4–O1–C1$_{Glc}$	3.17
	$^4C_1$	GlcN,6S	H1–C1–O5–C5	6.41
			H5–C1–O5–C1	1.28
			H1–C1–C2–C3	3.44
			H3–C3–C2–C1	1.16
			H1–C1–O1–C4$_{IdoA}$	0.81
2	$^2S_0$	IdoA2S	H1–C1–O5–C5	5.17
			H5–C1–O5–C1	3.37
			H1–C1–C2–C3	0.01
			H3–C3–C2–C1	0.01
			H4–C4–O1–C1$_{Glc}$	3.30
	$^4C_1$	GlcN,6S	H1–C1–O5–C5	5.88
			H5–C1–O5–C1	0.74
			H1–C1–C2–C3	2.25
			H3–C3–C2–C1	2.08
			H1–C1–O1–C4$_{IdoA}$	1.97

Two forms (**1** and **2**) correspond to different conformations ($^1C_4$ and $^2S_0$) of the IdoA2S residue. The GlcN,6S residue is in the $^4C_1$ form.

ent atomic charges, C1–O5 bond lengths and C1–O5–C5 bond angles seem to contribute to the above differences in coupling constants magnitudes. Relatively small magnitudes of computed proton–carbon interglycosidic $^3J_{H\text{-}1,C\text{-}1,O\text{-}1,C\text{-}4(IdoA)}$ coupling constants (0.81 Hz and 1.97 Hz, averaged value 1.05 Hz) are also interesting. Conversely, $^3J_{H\text{-}4,C\text{-}4,O\text{-}1,C\text{-}1(Glc)}$ magnitudes are larger and comparable each to other in both forms of the IdoA2S residue (3.17 and 3.30 Hz). $^3J_{H–C–C–C}$ magnitudes depend also upon stereoelectronic effects. In general, their contributions are smaller compared to $^3J_{H–C–O–C}$ coupling constants, but not negligible. About 1 Hz difference between $^3J_{H\text{-}1,C\text{-}1,C\text{-}2,C\text{-}3}$ (3.44 Hz compared to 2.25 Hz) in the GlcN,6S residues in **1** and **2** is noticeable as both torsion angles (H-1,C-1,C-2,C-3) are comparable (173° and −176°, respectively) to each other.

In summary, presented theoretical data demonstrate that DFT calculations at the B3LYP/6-311++G** level of theory offer good geometries of GAG compounds. The effects of sulfate and carboxylate groups upon the molecular geometry of heparin disaccharide can be examined by DFT using the high level basis set. The computed energies confirmed that more stable is disaccharide having the IdoA2S residue in the $^1C_4$ chair form. The results also showed that conformation of the IdoA2S residue influenced the geometry of the GlcN,6S ring, sodium coordination and hydrogen bonding. The changes in molecular geometry resulted in different magnitudes of spin–spin coupling constants in two forms of the disaccharide. Time-averaged $^3J_{H–C–C–H}$ magnitudes were in a good agreement with the published experimental data.

Acknowledgments

This research was supported by VEGA Grant No. 2/5075/25, APVT Grant No. 51-034504, and EU Grant No. QLK3-2002-02049.

References

1. Conrad, H. E. *Heparin-Binding Proteins*; Academic Press: San Diego, 1998.
2. *Heparin—Chemical and Biological Properties*; Lane, D. A., Lindahl, U., Eds.; CRC Press: Boca Raton, FL, 1989.
3. Mulloy, B.; Forster, M. J. *Glycobiology* **2000**, *10*, 1147–1156.
4. Casu, B.; Lindahl, U. *Adv. Carbohydr. Chem. Biochem.* **2001**, *57*, 159–208.
5. Capila, I.; Linhardt, R. J. *Angew. Chem., Int. Ed.* **2002**, *41*, 390–412.
6. Torri, G.; Casu, B.; Gatti, G.; Petitou, M.; Choay, J.; Jacquinet, J.-C.; Sinay, P. *Biochem. Biophys. Res. Commun.* **1985**, *128*, 134–140.
7. Ferro, D. R.; Provasoli, A.; Ragazzi, M.; Torri, G.; Casu, B.; Gatti, G.; Jacquinet, J. C.; Sinay, P.; Petitou, M.; Choay, J. *J. Am. Chem. Soc.* **1986**, *108*, 6773–6778.
8. Hricovíni, M.; Nieto, P. M.; Torri, G. In *NMR Spectroscopy of Glycoconjugates*; Jimenez-Barbero, J., Peters, T., Eds.; Wiley-VCH, 2002; pp 189–229.
9. Ragazzi, M.; Ferro, D. R.; Provasoli, A. *J. Comput. Chem.* **1986**, *7*, 105–112.
10. Forster, M. J.; Mulloy, B. *Biopolymers* **1993**, *33*, 575–588.
11. Angulo, J.; Nieto, P. M.; Martin-Lomas, A. *Chem. Commun.* **2003**, *13*, 1512–1513.
12. Ferro, D. R.; Provasoli, A.; Ragazzi, M.; Casu, B.; Torri, G.; Bossennec, V.; Perly, B.; Sinay, P.; Petitou, M.; Choay, J. *Carbohydr. Res.* **1990**, *195*, 157–167.
13. Casu, B.; Petitou, M.; Provasoli, A.; Sinay, P. *Trends Biochem. Sci.* **1988**, *13*, 221–225.
14. Mikhailov, D.; Linhardt, R. J.; Mayo, K. H. *Biochem. J.* **1997**, *328*, 51–61.
15. Mulloy, B.; Forster, M. J.; Jones, C.; Davies, D. B. *Biochem. J.* **1993**, *293*, 849–858.
16. Rabenstein, D. L.; Robert, J. M.; Peng, J. *Carbohydr. Res.* **1995**, *278*, 239–256.
17. Chevalier, F.; Lucas, R.; Angulo, J.; Martín-Lomas, M.; Nieto, P. M. *Carbohydr. Res.* **2004**, *339*, 975–983.
18. Ernst, S.; Venkataraman, G.; Sasisekharan, V.; Langer, R.; Cooney, C. L.; Sasisekharan, R. *J. Am. Chem. Soc.* **1998**, *120*, 2099–2107.
19. Lii, J.-H.; Ma, B.; Allinger, N. L. *J. Comput. Chem.* **1999**, *20*, 1593–1603.
20. Tvaroška, I.; Taravel, F. R.; Utille, J. P.; Carver, J. P. *Carbohydr. Res.* **2002**, *337*, 353–367.
21. Momany, F. A.; Appel, M.; Willett, J. L.; Schnupf, U.; Bosma, W. B. *Carbohydr. Res.* **2006**, *341*, 525–537.
22. Tissot, B.; Salpin, J. Y.; Martinez, M.; Gaigeot, M. P.; Daniel, R. *Carbohydr. Res.* **2006**, *341*, 598–609.
23. Scholzová, E.; Mach, P.; Hricovíni, M. *Molecules* **2003**, *8*, 770–779.
24. Hricovíni, M. . *Carbohydr. Res.* **2006**, *341*, 2575–2580.
25. Hricovíni, M.; Bizik, F. . *Carbohydr. Res.* **2007**, *342*, 779–783.

26. JAGUAR 3.5, Schrodinger, Inc., Portland, 1998.
27. Parr, R. G.; Wang, W. *Density-Functional Theory of Atoms and Molecules*; Oxford University Press: New York, 1994.
28. Lee, C.; Yang, W.; Paar, R. G. *Phys. Rev. B* **1988**, *37*, 785–789.
29. Becke, A. D. *J. Chem. Phys.* **1993**, *98*, 5648–5652.
30. Becke, A. D. *Phys. Rev. A* **1988**, *38*, 3098–3100.
31. Vosko, S. H.; Wilk, L.; Nusair, M. *Can. J. Phys.* **1980**, *58*, 1200–1208.
32. Frisch, M. J.; Trucks, G. W.; Schlegel, H. B.; Scuseria, G. E.; Robb, M. A.; Cheeseman, J. R.; Montgomery, J. A., Jr.; Vreven, T.; Kudin, K. N.; Burant, J. C.; Millam, J. M.; Iyengar, S. S.; Tomasi, J.; Barone, V.; Mennucci, B.; Cossi, M.; Scalmani, G.; Rega, N.; Petersson, G. A.; Nakatsuji, H.; Hada, M.; Ehara, M.; Toyota, K.; Fukuda, R.; Hasegawa, J.; Ishida, M.; Nakajima, T.; Honda, Y.; Kitao, O.; Nakai, H.; Klene, M.; Li, X.; Knox, J. E.; Hratchian, H. P.; Cross, J. B.; Bakken, V.; Adamo, C.; Jaramillo, J.; Gomperts, R.; Stratmann, R. E.; Yazyev, O.; Austin, A. J.; Cammi, R.; Pomelli, C.; Ochterski, J. W.; Ayala, P. Y.; Morokuma, K.; Voth, G. A.; Salvador, P.; Dannenberg, J. J.; Zakrzewski, V. G.; Dapprich, S.; Daniels, A. D.; Strain, M. C.; Farkas, O.; Malick, D. K.; Rabuck, A. D.; Raghavachari, K.; Foresman, J. B.; Ortiz, J. V.; Cui, Q.; Baboul, A. G.; Clifford, S.; Cioslowski, J.; Stefanov, B. B.; Liu, G.; Liashenko, A.; Piskorz, P.; Komaromi, I.; Martin, R. L.; Fox, D. J.; Keith, T.; Al-Laham, M. A.; Peng, C. Y.; Nanayakkara, A.; Challacombe, M.; Gill, P. M. W.; Johnson, B.; Chen, W.; Wong, M. W.; Gonzalez, C.; Pople, J. A.; GAUSSIAN 03, *Revision C.02*. Gaussian: Wallingford CT; 2004.
33. Godbout, N.; Salahub, D. R.; Andzelm, J.; Wimmer, E. *Can. J. Chem.* **1992**, *70*, 560–571.
34. Yates, E. A.; Mackie, W.; Lamba, D. *Int. J. Biol. Macromol.* **1995**, *17*, 219–223.
35. LaFerla, B.; Lay, L.; Guerrini, M.; Poletti, L.; Panza, L.; Russo, G. *Tetrahedron* **1999**, *55*, 9867–9880.